

Hybrid PV/fuel cell based system using integrated SEPIC-Cuk converter with crow search optimized PI controller

Yannam Ravi Sankar¹, Koritala Chandra Sekhar²

¹Department of Electrical and Electronics Engineering, Dr. YSR ANU College of Engineering and Technology, Acharya Nagarjuna University, Guntur, India

²Department of Electrical and Electronics Engineering, R.V. R. and J. C. College of Engineering, Guntur, India

Article Info

Article history:

Received Aug 8, 2023

Revised Dec 24, 2023

Accepted Jan 13, 2024

Keywords:

Battery
Boost converter
CS optimized PI controller
Fuel cell
Microgrid
PV system
SEPIC integrated Cuk converter

ABSTRACT

The study investigates a micro grid incorporating photovoltaic (PV), fuel cell and battery systems with an optimized proportional integral (PI) controller. A PV system serves as the primary green energy source, while a fuel cell acts as a supplementary source to compensate for power fluctuations. A single ended primary inductance converter (SEPIC) integrated Cuk converter boosts PV system's DC output voltage, controlled by a crow search-optimized PI (CS-PI) controller. A PI controller controls the fuel cell's minimum DC output voltage, which is raised by a boost converter to produce a controlled output. The proposed converter demonstrates robust performance across varying operational conditions with a reduced settling time of 0.9 s and an efficiency of 96.2%. A bidirectional converter links the battery to the grid, facilitating energy transfer in both directions and accommodating boost and buck operating characteristics thereby maintaining a state-of-charge (SOC) of 60%. This study employs MATLAB to establish effective PV-fuel storage control approaches, optimize energy extraction, and ensure steady power for a grid-connected system.

This is an open access article under the [CC BY-SA](https://creativecommons.org/licenses/by-sa/4.0/) license.



Corresponding Author:

Yannam Ravi Sankar
Department of Electrical and Electronics Engineering
Dr YSR ANU College of Engineering and Technology, Acharya Nagarjuna University
Namburu, Guntur, Andhra Pradesh 522510, India
Email: ravi.yannam2@gmail.com

NOMENCLATURE

| | | | |
|-------|---|-----|-------------------------------|
| PV | : Photovoltaic | FA | : Firefly algorithm |
| SEPIC | : Single ended primary inductance converter | PSO | : Particle swarm optimization |
| PI | : Proportional integral | GA | : Genetic algorithm |
| CS | : Crow search | GWO | : Grey Wolf Optimization |
| DC | : Direct current | PWM | : Pulse width modulation |
| SOC | : State-of-charge | AP | : Awareness of probability |
| MPP | : Maximum power point | FL | : Flight length |
| ABC | : Artificial bee colony | | |

1. INTRODUCTION

The increasing of renewable energy sources (RES) is a major imposition because of the declining value of conventional fossil fuel sources. Opting for renewable energy instead of fossil fuels offers numerous economic and environmental benefits. The majority of renewable energy sources are sustainable and

contributes minimally, if at all, to global warming emissions, as harness energy from natural resources. Additionally, RES operations and maintenance costs are significantly less than those of traditional fossil fuel plants [1]–[4]. Among all renewable sources, photovoltaic garnered the most attention due to their environmentally benign nature, safe, clean, portable behavior, and free accessibility. Nevertheless, the initial investment in setup and manufacturing is high, although it is going to decrease with examination and large-scale use [5]. The generated power from the photovoltaic (PV) module is affected by its surroundings, which cause power changes under changing operating circumstances. Consequently, the need for additional power sources like fuel cells, diesel generators, and batteries. Battery and diesel generators, respectively, have no ability to fulfill complete load demand and specific period backups. Solar energy production is affected by changes in air conditions because it is dependent on solar irradiance [6]–[8]. The fuel cell is a regulated supply that offers supplemental power and satisfies insufficient PV-power integration with important benefits such as high efficiency, extensibility and fuel adjustability [9]. When compared to alternative solutions, the on grid solar wind hydrogen energy system with battery storage had the lowest overall net present cost and cost of energy, according to the analysis of the various systems [10]–[13]. Hydrogen fuel cell is acknowledged as a key energy carrier in sustainable energy planning, poised to address ecological pollution issues arising from the utilization of fossil fuels [14]. It is also regarded as an eco-friendly technology due to its combustion-free process in generating electrical energy, resulting in the release of water as a byproduct [15].

Since the extensive accessibility of the limited supply of fossil fuels, the application of PV systems has expanded considerably. Furthermore, by generating zero greenhouse gases, the PV system helps to reduce warming temperatures [16], [17]. High voltage gain DC-DC converter is required to raise minimal output voltage produced by PV panels and provide controlled output under a variety of meteorological and solar irradiation conditions. To enhance the utility of RES, various types of converters should possess the capability to achieve substantial voltage changes with a high degree of amplification, all while adhering to specified quality standards [18], [19]. To achieve the appropriate amount of dc output voltage, several DC-DC converters are currently considered for PV applications. The Cuk converter features lower switching losses, increased voltage and more efficiency when carrying out maximum power point (MPP) actions when compared to other DC-DC converters like boost and buck boost. Likewise, the single ended primary inductance converter (SEPIC) converter produces non-inverted output with lower ripple content and handles a wide range of input voltages, generating it appropriate for uses where the input voltage may vary or needs to be regulated over a broad range [20]–[24]. However, traditional Cuk converters fail to provide the precise speed up/down voltage required for specific applications. As a result, in this study, a SEPIC integrated Cuk converter that functions in continuous conducting states as a steep voltage booster is proposed.

This system's electrical power production is improved by observing the highest power obtained by employing typical MPPT approaches such as P&O and incremental conductance, which are not always effective [25]. Because it is made for maximum power extraction, a closed loop control system with a PI controller is employed to increase an efficiency and dependability of maximum power extraction. The gain variables of PI controller are obtained by the application of numerous algorithms, the most common of which is trial and error, but it provides poor performance and degradation of the process throughout changes in load. Hence, the optimization is required to attain efficient system performance. Particle swarm optimization (PSO) [26], [27], firefly algorithm (FA) [28], genetic algorithm (GA) [29], [30], artificial bee colony (ABC) [31], and grey wolf optimization (GWO) [32], [33] are among algorithmic approaches proposed to enhance parameters of PI controller. The main drawbacks of PSO are the enormous number of iterations necessary for convergence, the divergence of high-speed particles and the lengthy convergence computational time. Nonetheless, the aforementioned algorithms are not capable of performing a speedy search of MPP with high convergence velocity, low computing load and low execution expense microcontroller. The crow search algorithm (CSA) is employed in the present research to enhance the functioning of the PI controller. It offers fast dynamic response with low convergence velocity.

When fuel as well as an oxidant are given, a fuel cell converts electrochemical energy and produces an electric current. Moreover, the output of fuel cell voltage is further enhanced with the support of a boost converter. It generates direct electricity by consuming hydrogen as fuel and emitting water and heat as contaminants. In a traditional PV production system, a battery is constantly attached to a DC bus [34]. Whenever the load changes rapidly without effective current management, the battery faces a potential threat. In this case, battery attached to DC bus using a bidirectional converter to control a decreasing current. The battery holds the necessary amount of electricity and sends surplus power to the DC microgrid when there is additional energy generation.

The hybrid energy setup that is the subject of this study includes a fuel cell that runs on hydrogen, a storage battery, and a photovoltaic system powered by the sun. A new contribution is proposed that uses an optimized PI controller with crow search to control the photovoltaic system's output voltage of a photovoltaic system via SEPIC integrated Cuk converter. The inclusion of a fuel cell along with boost converter as a supplementary source addresses power fluctuation in the micro grid. The fuel cell's role is to compensate for variations in power output from the PV system, contributing to overall grid stability. The bidirectional

converter linking the battery to the grid allows for energy transfer in both directions. To regulate energy supply, the storage device goes through charging and discharging operations. The proposed strategy is confirmed through MATLAB simulation and outcomes are generated.

2. PROPOSED SYSTEM DESCRIPTION

Figure 1 represents the proposed system diagram. Figure 1(a) displays a block diagram model of an efficient hybrid PV-FC system using optimized PI controller and Figure 1(b) displays a schematic diagram of proposed work. The generated DC output voltage from PV panel is subpar due to the unpredictability of the climate conditions. Hence, PV panel output is increased by using a SEPIC integrated Cuk converter.

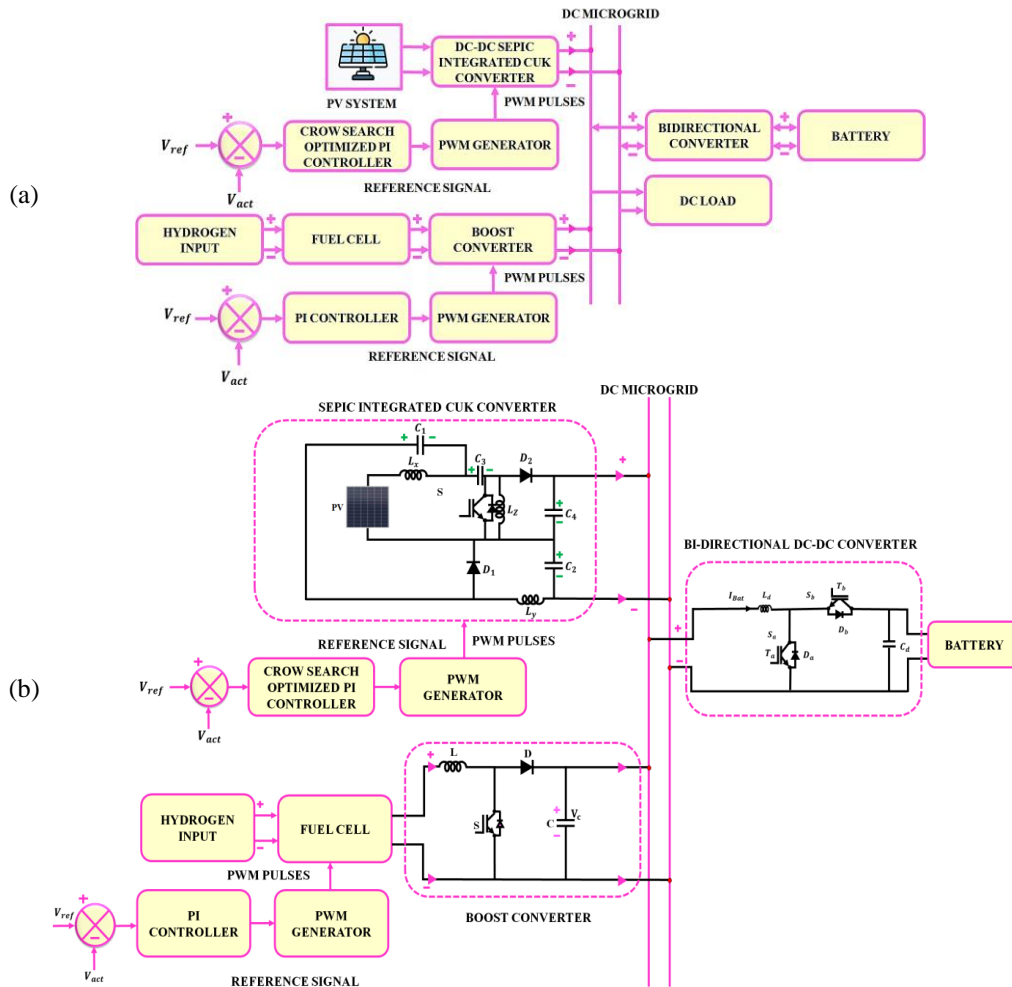


Figure 1. Proposed system: (a) an efficient hybrid PV-FC system using optimized PI controller and (b) schematic diagram of proposed work

The actual output voltage of converters is compared to the predicted reference value voltage to produce an error signal. PI controller with crow search optimization evaluates the acquired error signal and provides a reference control signal that instructs pulse width modulation (PWM) generator to begin generating gating pulses. The proposed converter's conversion efficiency is controlled by the gating pulses of PWM generator, which provide a controlled DC voltage. A boost converter is utilized to increase the DC voltage that is produced when hydrogen fuel is delivered into the fuel cell. The PWM generator receives an error signal from PI controller when the actual DC voltage of the converter differs from a reference voltage. PWM pulses produced by the PWM generator, which give an adequate DC voltage, control the boost converter's switching mechanism. It is necessary to have an appropriate battery system to preserve the excess energy generated. Use of a bi-directional DC to DC converter provides the required bidirectional flow of power for battery discharging

and charging. Lastly, a constant and uninterrupted power supply is given to the DC load. Block diagram for proposed work appears in Figure 1(b).

3. PROPOSED SYSTEM MODELLING

3.1. PV system modelling

A comparable PV cell constructed with P-N junction is shown in Figure 2. To create a PV module, multiple series and shunt interconnections of PV cells have to be built with consideration for the ambient temperature and solar irradiation. The PV cell model's mathematical relationship is written as (1) and (2).

$$\begin{cases} I_{Out} = I_{Photon} - I_{Diode} - I_{Parallel} \\ \text{Where, } I_{Diode} = I_{Sat} \left[e^{\left(\frac{V_{Diode}}{m_D V_{TH}}\right)} - 1 \right] \end{cases} \quad (1)$$

$$\left. \begin{aligned} V_{Diode} &= V_{out} + I_{out} R_{series} \\ V_{TH} &= \frac{K_B T_{Abs}}{Q_{electron}}, I_{Parallel} = \frac{V_{Diode}}{R_{Parallel}} \end{aligned} \right\} \quad (2)$$

Where, I_{Out} stands for PV cell output current; $I_{Parallel}$ is current via a parallel resistor, I_{Photon} is current through a photon, I_{Diode} is current through a diode. Diode saturation current is I_{Sat} ; V_{out} is the resultant voltage, V_{Diode} is voltage across the diode, V_{TH} is the thermal voltage, m_D is the diode factor and K_B is Boltzmann constant. R_{series} is series resistance; The absolute temperature is T_{Abs} ; $R_{Parallel}$ is resistance in parallel, while $Q_{electron}$ is charge on an electron. For the purpose of increasing the PV panel voltage, an appropriate DC to DC converter is required, therefore this research uses a SEPIC-Cuk converter to produce a high dc output voltage. The forthcoming section provides a deep explanation of the proposed converter.

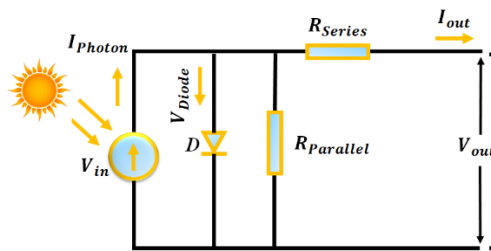


Figure 2. PV cell circuit

3.2. SEPIC-Cuk converter modelling

The proposed SEPIC integrated Cuk shown in Figure 3 effectively boosts the resultant voltage of the solar panel and eliminates a large amount of distortion. With non-inverted inputs, it offers outstanding performance by combining the advantages of the SEPIC and Cuk converters. This integration is typically achieved by using shared components, such as an inductor or a capacitor, to simplify the circuit while maintaining the advantages of both SEPIC and Cuk converters. Its design flexibility and applicability to a wide range of input voltages make it suitable for various power electronics applications. Additionally, the SEPIC-Cuk converter provides isolation between the input and output, which might be desirable for safety and control purposes in a PV system. Figure 4 presents the waveform's modes of operation for the SEPIC integrated Cuk converter.

Figure 5 exhibits the Cuk integrated SEPIC's circuitry, and the several modes of operation are described as:

- Mode 1 $[0 - t_a]$: During time $t = 0$ in mode 1 of Figure 5(a), the switch S becomes ON , charging the inductors L_x, L_y and L_z until time t_b . In this state, the diodes D_1, D_2 conduct inhibiting action while taking into consideration the voltages V_{C1} and V_{C4} , causing the capacitor C_1 to lose power via the switch S and the inductor L_y .
- Mode 2 $[t_a - t_b]$: When the control switch S gets switched off in mode 2, shown in Figure 5(b), as indicated, at time $t = t_a$, the voltage V_{C4} over the capacitance C_4 is higher than the voltage V_{C2} . As a result, after the time period t_a , the capacitance C_1 charges and the inductors L_x, L_y gets released. The diode D_1 switches to conduction mode between the times $t_a - t_b$ because the diode D_2 is still operating in reverse bias mode.

- Mode 3 $[t_b - t_c]$: In this state switch is still in its OFF condition in mode 3, as shown in Figure 5(c) and the voltage V_{C4} is identical to or lower than V_{C1} . Via the inductance L_x , the capacitors C_4, C_1 , and the inductors L_x, L_y , and L_z get charged up. As a result, the diodes D_1 and D_2 conduct current while delivering it to the load.

A suitable optimization approach must be used to control the proposed converter's operation while consistently maintaining DC link voltage. The following provides an overview of the optimization method employed in this research.

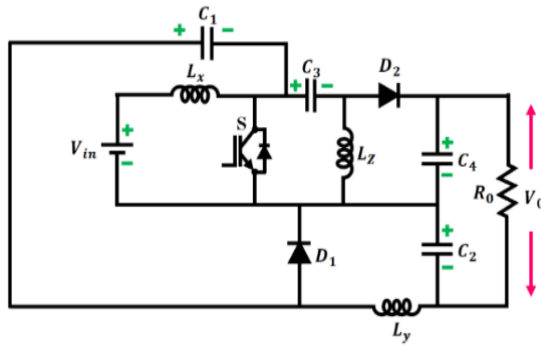


Figure 3. Proposed SEPIC-integrated Cuk converter

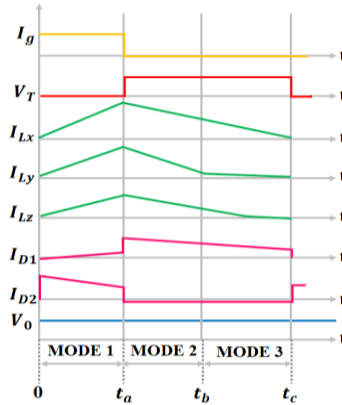


Figure 4. Conceptual waveform of proposed converter

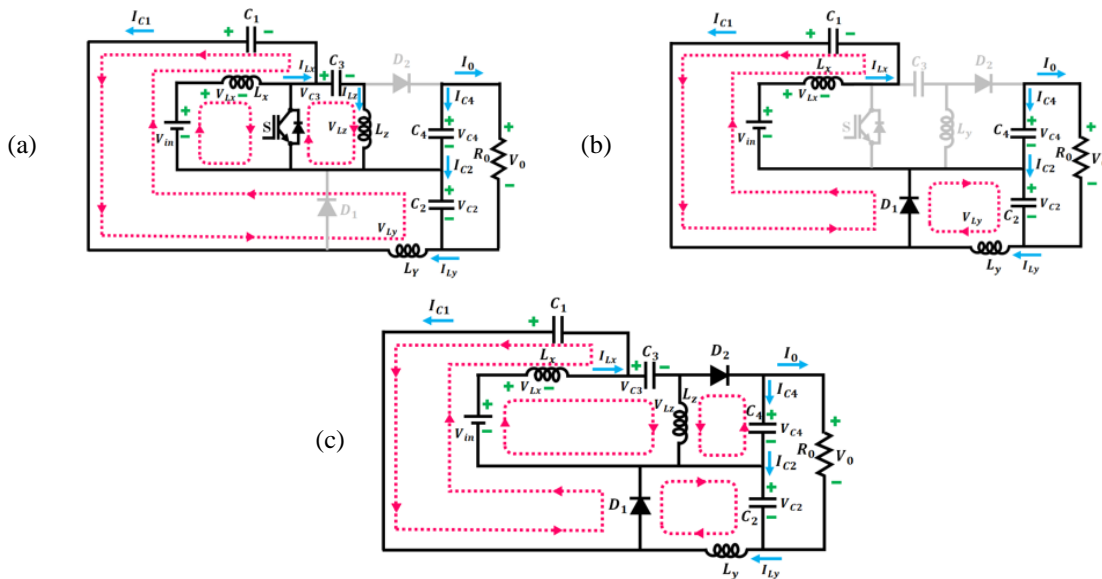


Figure 5. Modes of operation: (a) mode 1, (b) mode 2, and (c) mode 3

3.3. Crow search optimized PI controller

This metaheuristic method evolved using observations of crow intelligence and consciousness. Crows belong to the smartest birds because, in comparison to their size, their brains are larger. Crows often exhibit traits such as living in flocks, having an excellent memory, being follower thieves and having strong defensive skills. This behavior-based framework is used to frame the technique for deriving K_p and K_i . Awareness of probability (AP) is managed to keep concentration and diversity in a more balanced state. By reducing the value of AP, this method successfully finds an ideal solution that causes concentration to rise. The flow chart and the CS method's phases are highlights as in Figure 6. Every crow in a given flock is taken to be considered a potential solution in this process and the matrix is constructed accordingly.

$$Crows = \begin{bmatrix} x_1^1 & x_2^1 & \dots & x_d^1 \\ x_1^2 & x_2^2 & \dots & x_d^2 \\ \vdots & \vdots & \ddots & \vdots \\ x_1^F & x_2^F & \dots & x_d^F \end{bmatrix} \tag{3}$$

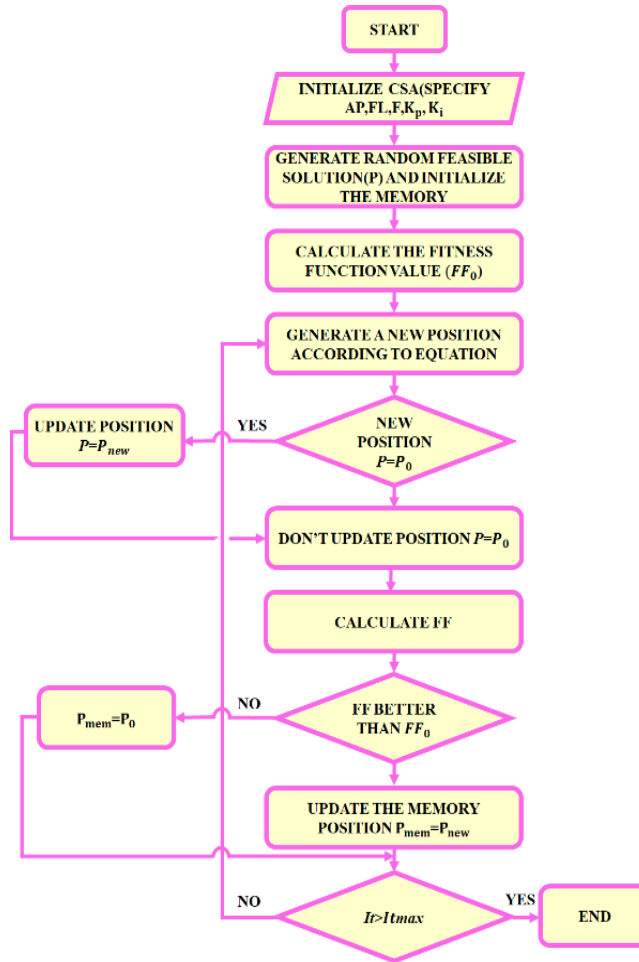


Figure 6. CS optimized PI controller

In this section the flock size and the decision variables are indicated by the letters d and F, correspondingly. Define the limitations, choices and issue. Initialize the CS parameters F, FL (flight length), AP, it_{max} (iterations number), K_p and K_i . With regard to it the amount of iterations and i number of crows ($i = 1, 2, \dots, F$), as shown in (4).

$$x^{i,it} = x_1^{i,it}, x_2^{i,it}, x_3^{i,it}, \dots, x_d^{i,it} \tag{4}$$

Consider that the food is in its starting position, which serves as the basis for initializing the memory.

$$mem = \begin{bmatrix} m_1^1 & m_2^1 & \dots & m_d^1 \\ m_1^2 & m_2^2 & \dots & m_d^2 \\ \vdots & \vdots & \ddots & \vdots \\ m_1^F & m_2^F & \dots & m_d^F \end{bmatrix} \tag{5}$$

The starting point of the crow is determined for each row by calculating the fitness value while taking the choice variables into account. The ith crow pursues the jth crow in search of the concealed food (m^j) when new position of the ith crow is determined based on a random crow j. The ith crow's new location is now indicated as (6).

$$x^{j,it} = x^{i,it} + r_j * (m^{j,it} - x^{i,it}) \quad (6)$$

The possible values of the random number in this case are [0, 1] and it is indicated as r_j . If feasible, the position is changed after checking for updates, otherwise the crow stays in its original location. According to (7), estimate fitness for the updated position and update memory.

$$m^{j,it} = x^{i,it} * f(x^{i,it}) \quad (7)$$

If the updated fitness value, determined by (7) compares favorably to the previously memorized one, the crow adjusts its location.

When the iteration reaches its maximum or an ideal solution is found, the revised fitness function and memory updating process are repeated. The K_p and K_i are set to their ideal levels using this procedure. The CS-PI controller employs the crow search algorithm to dynamically tune parameters of the PI controller in a micro grid system. Tuning process begins with the initialization of the PI parameters, which serve as the initial positions in the CSA's search space. The CSA, inspired by the cooperative and competitive behaviors of crows, guides the iterative optimization process. Crows, representing different sets of PI parameters, explore the search space to find optimal configurations that minimize a predefined objective function, capturing key performance criteria such as overshoot and settling time. Crow fitness in the search space is determined by evaluating each crow's fitness using an objective function. Through successive iterations, the algorithm refines the positions of the crows, reflecting adjustments to the PI parameters. The iterative nature of CSA allows for a dynamic exploration of the parameter space, eventually converging to a set of PI parameters that optimize the microgrid control system's performance under varying conditions. This adaptive and nature-inspired approach enhances the robustness and efficiency of the PI controller for effective regulation within the microgrid.

3.4. Fuel cell

A fuel cell uses an electrochemical energy conversion process to produce electricity when supplied with fuel. It generates green electricity and has the capacity to more effectively transform the chemical power of fuel into electrical power. It consists of an electrolytic solution, a cathode (a negative electrode), and an anode (a positive electrode).

In the process of being ionized at the anode, hydrogen gas releases electrons and produces H⁺ ions (or protons), as will be explained further down. This reaction results in the production of energy.



The interaction of oxygen with e⁻ ions from electrodes and H⁺ ions from electrolytes at the cathode results in the formation of water.



DC microgrid is connected to fuel cells using a boost converter, which increases output voltage level of fuel cell.

3.5. Boost converter

In broad terms, the fuel cell uses a boost converter for converting electrochemical energy into DC voltage. The boost converter is commonly chosen for fuel-cell systems due to an inherent characteristics of fuel cell voltage profiles. Fuel cells typically operate within a specific voltage range, and a boost converter is well-suited to increase an output voltage to desired level. By using a boost converter for fuel cell generator, the system efficiently raises the minimum DC output voltage of fuel cell to meet a requirement of the micro grid. Figure 7 represents the circuit diagram of proposed converter. Figure 7 (a) shows boost converter's circuit diagram.

The power switch is used by this converter and the circuitry operates in two stages. When switch is tuned ON at $t = 0$, phase-1 gets started. Via L and switch, the current flows continuously as mentioned in Figure 7(b). While the switch is deactivated at $t = t_1$, phase-2 begins as seen in Figure 7(c). Now, power switch current is flow via L, C , the load and diode D before returning to the IGBT. Until the switch is engaged in the succeeding cycle, the inductance current declines. The inductance L 's energy is transferred to the load.

3.6. Battery system using DC-DC bidirectional converter

A continuous flow of electrical power is necessary for the storage system's energy conversion process. To achieve this, the control system uses a bidirectional DC to DC chopper. Figure 8 depicts the converter's design for the current topic. The DC to DC converter is made up of two regulated toggle switches S_a and S_b , an inductive component, L_d and a filtering capacitor C_d . A converter combines two common circuits of electrical chopping: a step-down and a step-up chopper. While power source is being powered up, the bidirectional DC/DC

converter permits operation in both the power phase and regenerating mode. An appropriate control system generates a pair of signals to govern the converter's driven transistor switches. Using the bidirectional DC to DC converter's control mechanism, power from the battery can be managed. Suitable methods for charging and draining the battery bank have been successfully devised under this converter's supervision.

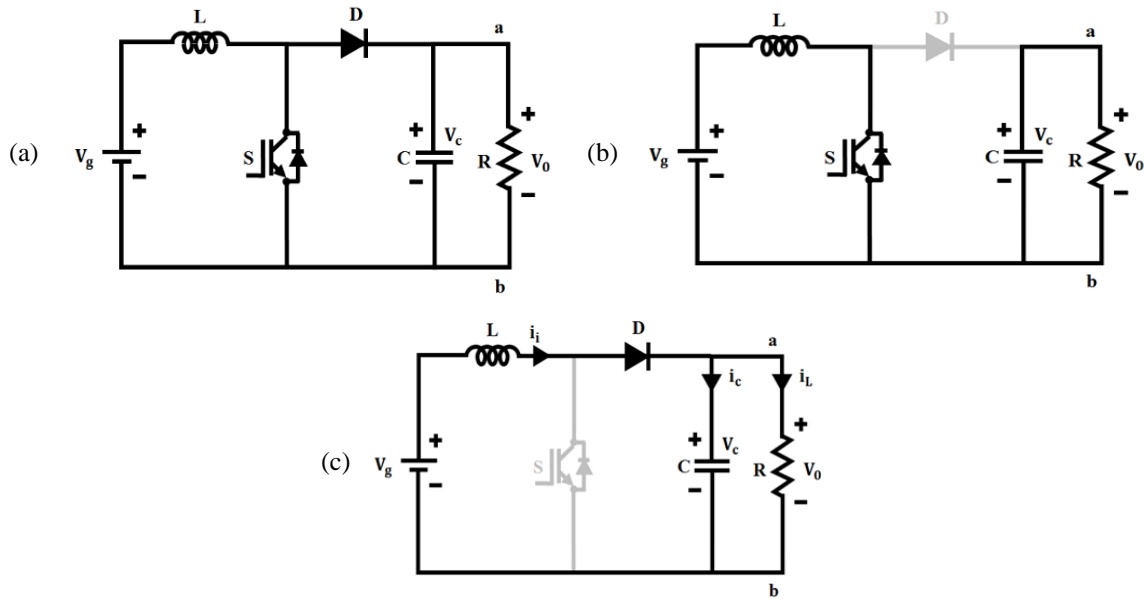


Figure 7. Illustration of circuit diagram: (a) boost converter, (b) mode 1 operation, and (c) mode 2 operation

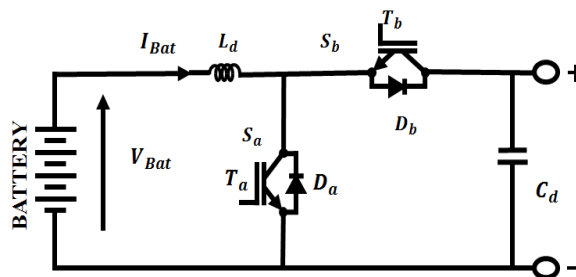


Figure 8. DC-DC bidirectional converter

4. RESULTS AND DISCUSSION

This work focuses on sustaining the hybrid energy system-based voltage consistency of the DC microgrid. In order to integrate fuel cell, battery and PV system into DC microgrid, a Cuk integrated SEPIC converter, a bidirectional converter and a battery are each used. The crow search optimized PI controller is utilized to govern the effectiveness of DC-DC converters with the goal of enhancing and managing the DC voltage. The effectiveness of this DC microgrid powered by a hybrid energy source is confirmed using MATLAB simulation. Table 1 displays the proposed system's parameter specifications.

Table 1. Parameter specifications

| | Parameters | Values |
|-----------------------------|---|------------------|
| PV panel | Peak power | 100 W, 15 Panels |
| | Short circuit current I_{SC} | 5.86 A |
| | Open circuit voltage V_{OC} | 22.68 V |
| | Number of series connected PV cells N_s | 36 |
| Fuel cell (full stack type) | Output current | 11.11 A |
| | Output voltage | 90 V |
| | Output power | 1 kW |
| SEPIC integrated Luo | Switching frequency f_s | 10 KHz |
| | L_x, L_y, L_z | 0.288 mH |
| | C_1, C_2, C_3, C_4 | 150 μ F |

Figures 9(a) and 9(b) illustrate the generated waveforms that indicate fluctuations in solar irradiation and temperature. Temperature increases from 25 °C to 35 °C in 0.25 seconds and PV panel irradiation output correspondingly increases from 800 W/m² to 1000 W/m² in 0.26 seconds. The rapid fluctuation in temperature and irradiation levels could be indicative of changing weather conditions, such as the passage of clouds or other atmospheric factors. An increase in irradiation directly impacts the amount of energy that the PV panel can convert into electricity.

In response to the variations in temperature and solar irradiation, an output current and voltage of PV panel exhibits variations as indicated in Figures 10(a) and 10(b). PV voltage increases from 65 V to 80 V indicating a positive correlation between solar irradiation levels and the output voltage. Similarly, the current shows an abrupt increase from 145 A to 175 A. Higher temperatures generally result in greater electron mobility within the semiconductor material of the PV cells, allowing for more efficient movement of charge carriers and an increase in current.

SEPIC-Cuk converter's output voltage with the related PI and CS-PI controllers is shown in Figure 11. Figure 11(a) represents converter output voltage using PI controller, which achieves 600 V after 0.4 s, similarly the Figure 11(b) represents converter output voltage using CS optimized PI controller which achieves constant 600 V with fast settling time (0.1 s). Figures 11(c) and 11(d) represents the outputs attained using genetic algorithm (GA) based PSO based PI controller and PI controller. By optimizing the PI controller parameters, CSO aims to reduce overshooting and oscillations, leading to a faster response and quicker attainment of the desired output. It continuously refines the controller parameters based on the system's real-time behavior.

Figure 12 indicates the output current waveform of proposed converter. The proposed converter provides a constant current of 3 A in spite of its initial fluctuations. The proposed control algorithm ensures that the output current is not only regulated but also responds quickly to changes, providing a stable and constant current output. Figure 13 shows that the output voltage waveform of the fuel cell consistently maintains 480 V.

Output waveforms of fuel cell-based boost converter is demonstrated in Figure 14, from this observation, it is evident that constant input current 100 A is maintained after 0.34 sec as indicated in Figure 14(a). Correspondingly, a stable output voltage and current of 600 V and 48 A are maintained as indicated in Figures 14(b) and 14(c) respectively. The PV system along with the fuel cell together aids in supplying a constant uninterrupted energy supply to the DC microgrid.

The representations of the battery current, voltage and SOC are displayed in Figures 15(a)-15(c), correspondingly. A battery's SOC, which is represented in percentage, is the amount of charge it holds in relation to its capability. When the SOC number is less than 60% and more than 60%, the battery gets charged and discharged, respectively. Here, the constant battery voltage 125 V is obtained and current become stable after 0.6 sec with minor distortions.

Table 2 and Figure 16 denotes the comparison analysis of proposed converter efficiency with different converter, such as boost, Cuk, and SEPIC. The efficiency of the SEPIC integrated Cuk converter is 96.2% which is considerably higher than the other three converters. The combined features of the SEPIC and Cuk converter contribute to enhanced voltage regulation with reduced fluctuations.

Figure 17 denotes the comparison evaluation of convergence speed. From plot, it is evident that, proposed CS-PI controller attains faster convergence speed. From the Table 3 observation, compared to conventional PI controller, the proposed CS optimized PI controller outperforms in case of rise time t_r , settling time t_s and peak time t_p . Proposed optimized PI controller achieves quick settling time, which is given by 0.1 seconds. The optimization process carried out by CSO is geared towards enhancing the control system's overall performance, with a specific focus on achieving a faster and more accurate response resulting in a more stable and efficient control system.

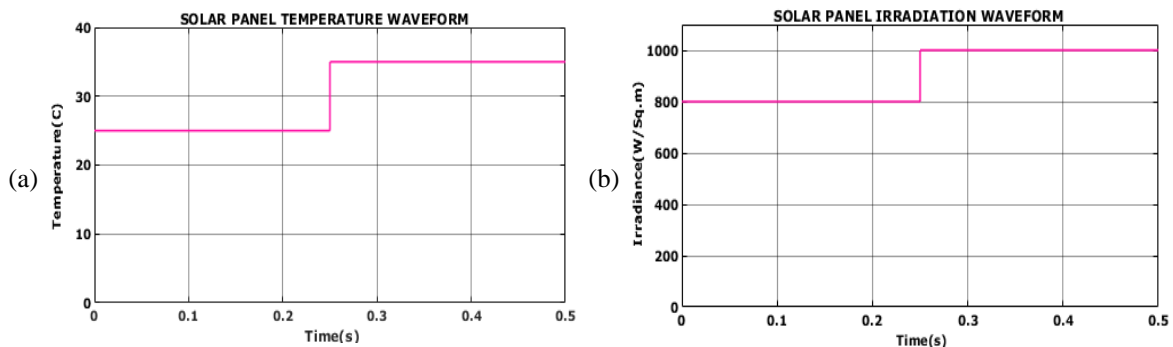


Figure 9. Waveforms for system: (a) temperature and (b) irradiation

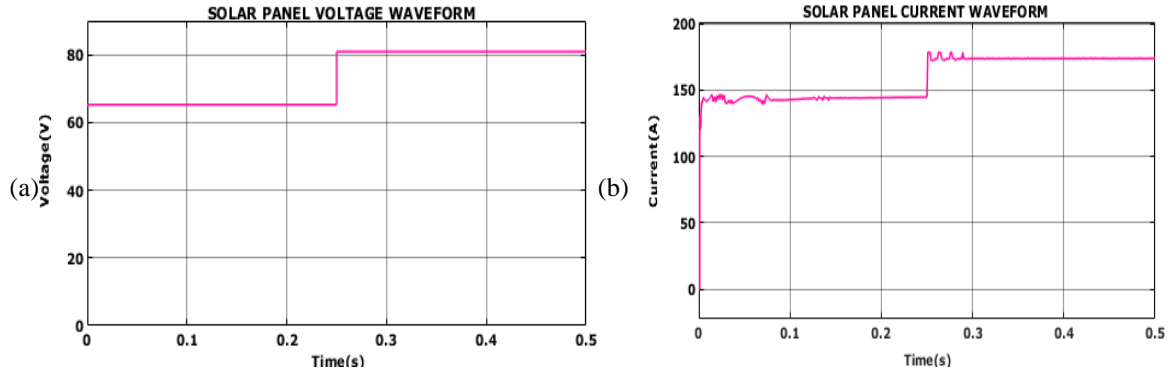


Figure 10. Waveforms for PV panel: (a) voltage and (b) current

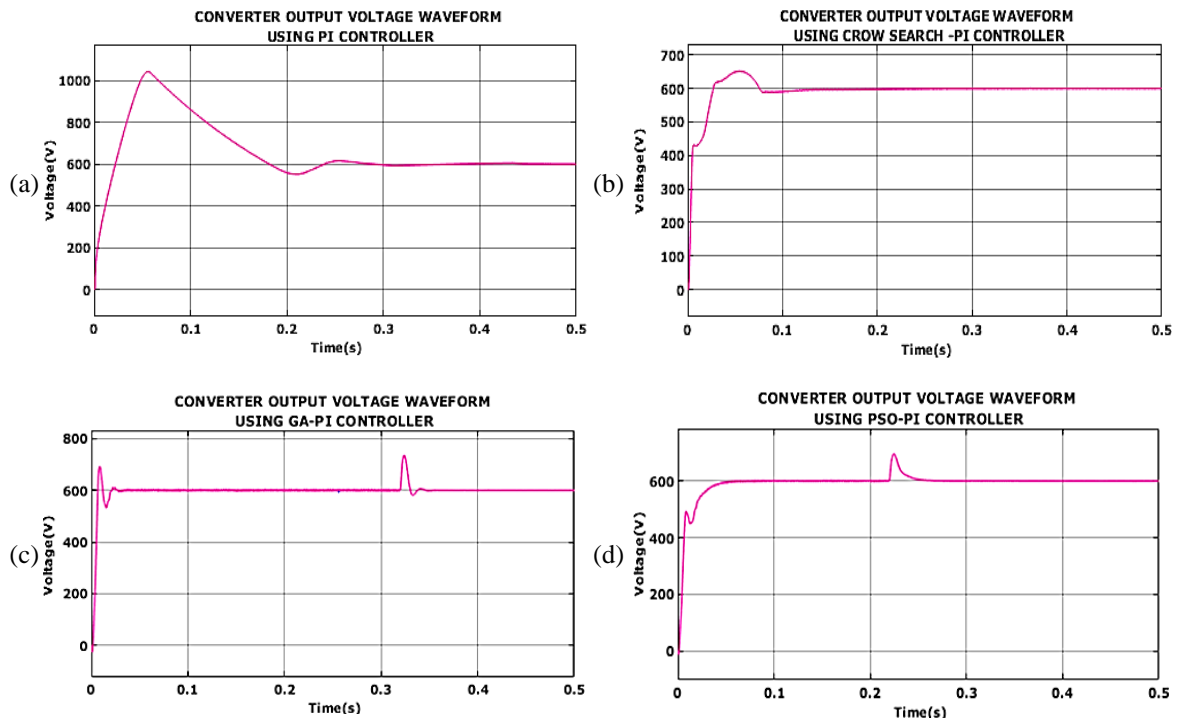


Figure 11. Waveforms for SEPIC-Cuk converter output voltage: (a) using PI controller, (b) using CS-PI controller, (c) using GA-PI controller, and (d) using PSO-PI controller

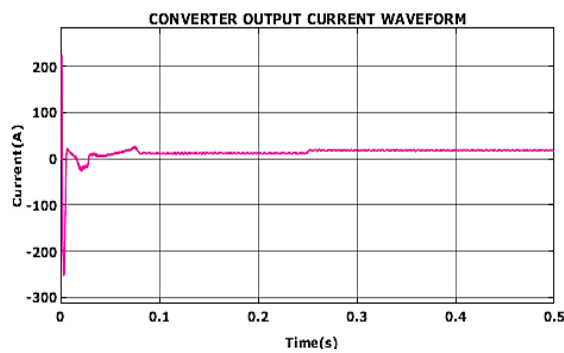


Figure 12. Converter output current waveform

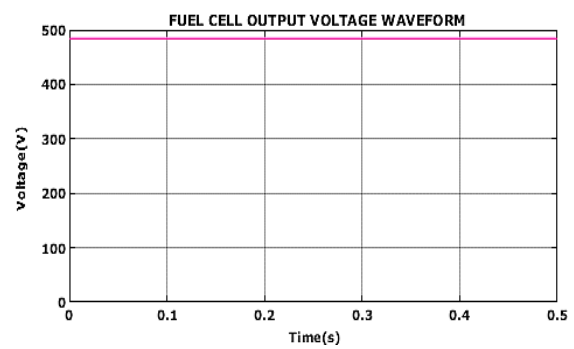


Figure 13. Output voltage of fuel cell

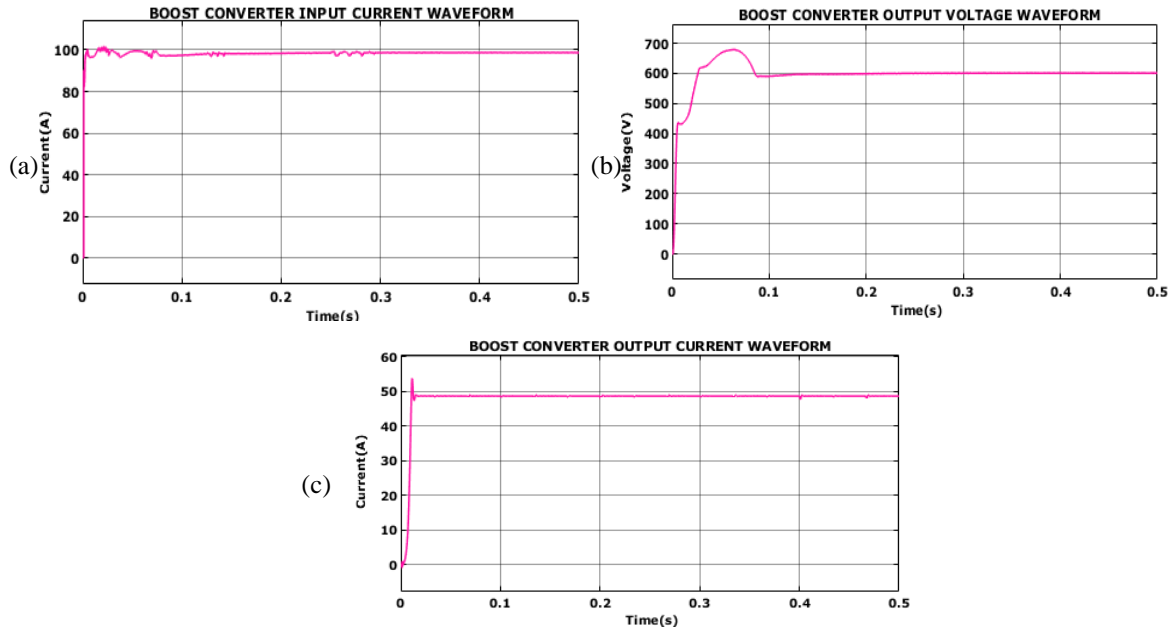


Figure 14. Waveforms of fuel cell-based boost converter: (a) input current, (b) output voltage, and (c) output current

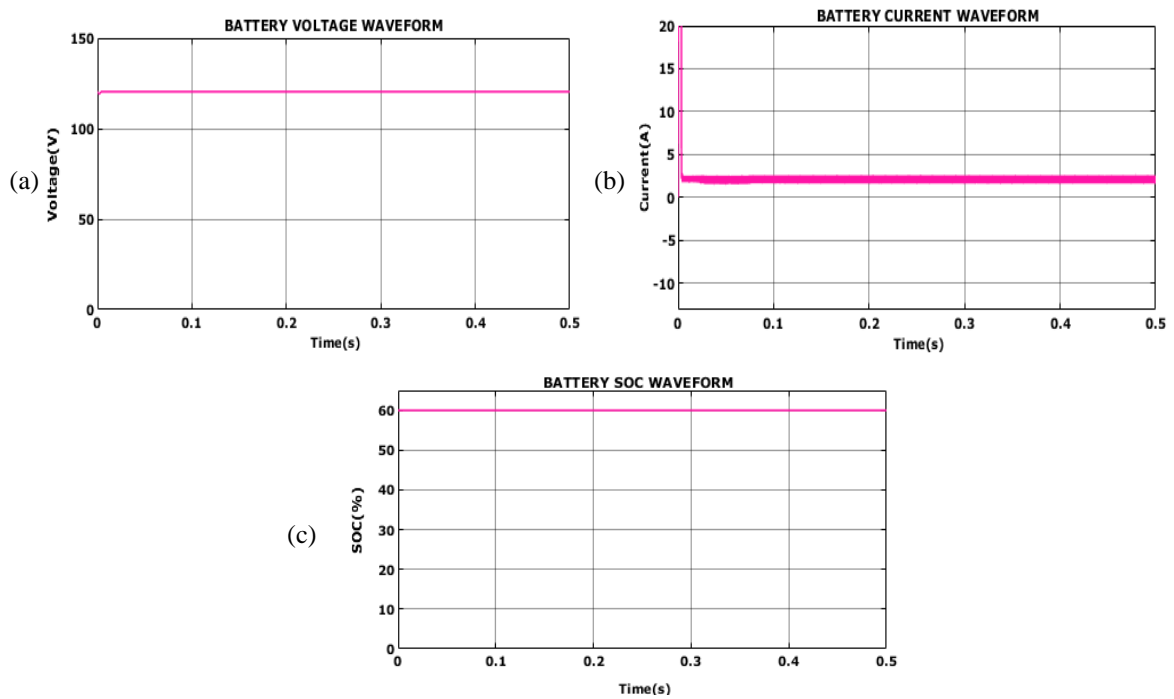


Figure 15. Output waveforms for battery: (a) voltage, (b) current, and (c) SOC

Table 2. Comparison analysis of efficiency

| Converters | Efficiency (%) |
|----------------------|----------------|
| Boost [35] | 80 |
| Cuk [36] | 85 |
| SEPIC [37] | 88.82 |
| SEPIC integrated Cuk | 96.2 |

Table 3. Comparison analysis of controller

| | Rise time t_r (s) | Peak time t_p (s) | Settling time t_s (s) |
|-------------------|------------------------|------------------------|----------------------------|
| PSO-PI controller | 0.01 | 0.05 | 0.28 |
| GA-PI controller | 0.01 | 0.02 | 0.36 |
| PI controller | 0.06 | 0.08 | 0.45 |
| CS-PI controller | 0.03 | 0.07 | 0.1 |

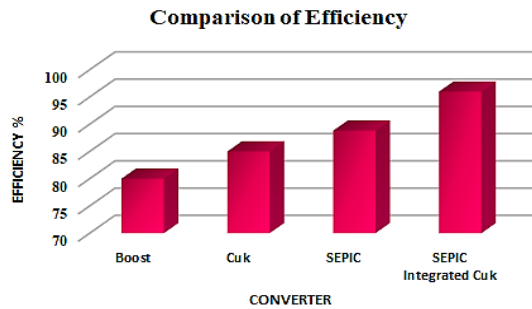


Figure 16. Comparison analysis of efficiency

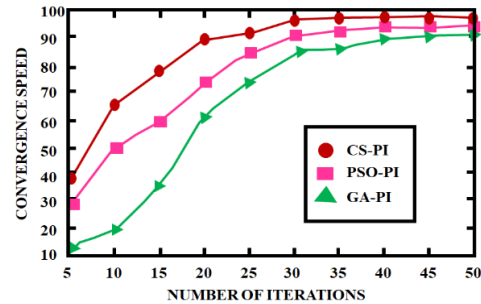


Figure 17. Comparison analysis of convergence speed

5. CONCLUSION

In this work, hybrid PV, fuel cell, and battery systems are examined employing a PI controller that has been optimized by crow search algorithm for a DC microgrid system. In order to balance out power shortages, a fuel cell serves in addition to PV; however, solar panel remain the main sustainable power source. A SEPIC integrated Cuk converter is utilized to enhance PV system's minimum DC output voltage, and CS-PI controller is utilized to control converter's function of operation to provide an optimal output. A rapid PV observation with no change around the MPP is also made possible by the CS optimized PI controller. The fuel cell's lowest DC voltage is raised by a boost converter, and its operation is regulated by a PI controller to provide a controlled output. According to simulation results, suggested converter has a high efficiency of 96.2% and outperforms other existing converters. The proposed controller generates reduced settling time of 0.1s which is comparatively lower than conventional PI controller.




REFERENCES

- [1] N. Alshammari, M. M. Samy, and J. Asumadu, "Optimal Economic Analysis Study for Renewable Energy Systems to Electrify Remote Region in Kingdom of Saudi Arabia," *2018 20th International Middle East Power Systems Conference, MEPCON 2018 - Proceedings*, pp. 1040–1045, 2018, doi: 10.1109/MEPCON.2018.8635287.
- [2] A. F. Tazay, M. M. Samy, and S. Barakat, "A Techno-Economic Feasibility Analysis of an Autonomous Hybrid Renewable Energy Sources for University Building at Saudi Arabia," *Journal of Electrical Engineering and Technology*, vol. 15, no. 6, pp. 2519–2527, 2020, doi: 10.1007/s42835-020-00539-x.
- [3] M. B. Eteiba, S. Barakat, M. M. Samy, and W. I. Wahba, "Optimization of an off-grid PV/Biomass hybrid system with different battery technologies," *Sustainable Cities and Society*, vol. 40, pp. 713–727, 2018, doi: 10.1016/j.scs.2018.01.012.
- [4] M. M. Samy, M. I. Mosaad, M. F. El-Naggar, and S. Barakat, "Reliability Support of Undependable Grid Using Green Energy Systems: Economic Study," *IEEE Access*, vol. 9, pp. 14528–14539, 2021, doi: 10.1109/ACCESS.2020.3048487.
- [5] V. F. Pires, A. Cordeiro, D. Foito, and J. F. A. Silva, "Dual Output and High Voltage Gain DC-DC Converter for PV and Fuel Cell Generators Connected to DC Bipolar Microgrids," *IEEE Access*, vol. 9, pp. 157124–157133, 2021, doi: 10.1109/ACCESS.2021.3122877.
- [6] K. S. Kavin, P. Subha Karavelam, A. Pathak, T. R. Premila, R. Hemalatha, and T. Kumar, "Modelling and Analysis of Hybrid Fuzzy Tuned PI Controller based PMBLDC Motor for Electric Vehicle Applications," *SSRG International Journal of Electrical and Electronics Engineering*, vol. 10, no. 2, pp. 8–18, 2023, doi: 10.14445/23488379/IJEEE-V10I2P102.
- [7] E. Ka, Thomas Thangam, and K. Muthuvel, "SEPIC Converter with Closed Loop PI Controller for Grid Utilized PV System," *Journal of Next Generation Information Technology*, vol. 1, no. 1, pp. 16–28, 2021.
- [8] P. Prabhakaran and V. Agarwal, "Novel Four-Port DC-DC Converter for Interfacing Solar PV-Fuel Cell Hybrid Sources with Low-Voltage Bipolar DC Microgrids," *IEEE Journal of Emerging and Selected Topics in Power Electronics*, vol. 8, no. 2, pp. 1330–1340, 2020, doi: 10.1109/JESTPE.2018.2885613.
- [9] P. Andrade, A. N. Alcaso, F. Bento, and A. J. Marques Cardoso, "Buck-Boost DC-DC Converters for Fuel Cell Applications in DC Microgrids—State-of-the-Art," *Electronics (Switzerland)*, vol. 11, no. 23, 2022, doi: 10.3390/electronics11233941.
- [10] S. Barakat, M. M. Samy, M. B. Eteiba, and W. I. Wahba, "Viability study of grid connected PV/Wind/Biomass hybrid energy system for a small village in Egypt," *2016 18th International Middle-East Power Systems Conference, MEPCON 2016 - Proceedings*, pp. 46–51, 2017, doi: 10.1109/MEPCON.2016.7836870.
- [11] C. Mokhtara, B. Negrou, N. Settou, B. Settou, and M. M. Samy, "Design optimization of off-grid Hybrid Renewable Energy Systems considering the effects of building energy performance and climate change: Case study of Algeria," *Energy*, vol. 219, 2021, doi: 10.1016/j.energy.2020.119605.
- [12] M. M. Samy, H. I. Elkhoully, and S. Barakat, "Multi-objective optimization of hybrid renewable energy system based on biomass and fuel cells," *International Journal of Energy Research*, vol. 45, no. 6, pp. 8214–8230, 2021, doi: 10.1002/er.5815.
- [13] S. Barakat, M. M. Samy, M. B. Eteiba, and W. I. Wahba, "Feasibility Study of Grid Connected PV-Biomass Integrated Energy System in Egypt," *International Journal of Emerging Electric Power Systems*, vol. 17, no. 5, pp. 519–528, 2016, doi: 10.1515/ijeeps-2016-0056.
- [14] M. M. Samy, S. Barakat, and H. S. Ramadan, "A flower pollination optimization algorithm for an off-grid PV-Fuel cell hybrid renewable system," *International Journal of Hydrogen Energy*, pp. 2141–2152, 2019, doi: 10.1016/j.ijhydene.2018.05.127.
- [15] D. Çalşır, S. Ekici, A. Midilli, and T. H. Karakoc, "Benchmarking environmental impacts of power groups used in a designed UAV: Hybrid hydrogen fuel cell system versus lithium-polymer battery drive system," *Energy*, vol. 262, 2023, doi: 10.1016/j.energy.2022.125543.
- [16] S. Vasantharaj, V. Indragandhi, V. Subramaniaswamy, Y. Teekaraman, R. Kuppasamy, and S. Nikolovski, "Efficient control of dc microgrid with hybrid pv—fuel cell and energy storage systems," *Energies*, vol. 14, no. 11, 2021, doi: 10.3390/en14112324.
- [17] S. Manna *et al.*, "Design and implementation of a new adaptive MPPT controller for solar PV systems," *Energy Reports*, vol. 9, pp. 1818–1829, 2023, doi: 10.1016/j.egy.2022.12.152.




- [18] B. Melzi, N. Kefif, M. El Haj Assad, H. Delnava, and A. Hamid, "Modelling and optimal design of hybrid power system photovoltaic/solid oxide fuel cell for a mediterranean city," *Energy Engineering: Journal of the Association of Energy Engineering*, vol. 118, no. 6, pp. 1767–1781, 2021, doi: 10.32604/EE.2021.017270.
- [19] R. A. Khan, H. D. Liu, C. H. Lin, S. Der Lu, S. J. Yang, and A. Sarwar, "A Novel High-Voltage Gain Step-Up DC–DC Converter with Maximum Power Point Tracker for Solar Photovoltaic Systems," *Processes*, vol. 11, no. 4, 2023, doi: 10.3390/pr11041087.
- [20] P. Wang, L. Zhou, Y. Zhang, J. Li, and M. Sumner, "Input-Parallel Output-Series DC-DC Boost Converter with a Wide Input Voltage Range, for Fuel Cell Vehicles," *IEEE Transactions on Vehicular Technology*, vol. 66, no. 9, pp. 7771–7781, 2017, doi: 10.1109/TVT.2017.2688324.
- [21] M. R. Banaei and H. A. F. Bonab, "A High Efficiency Nonisolated Buck-Boost Converter Based on ZETA Converter," *IEEE Transactions on Industrial Electronics*, vol. 67, no. 3, pp. 1991–1998, 2020, doi: 10.1109/TIE.2019.2902785.
- [22] B. Chandrasekar, N. Chellammal, and B. Nallamothu, "Non-isolated unidirectional three-port cuk-cuk converter for fuel cell/solar pv systems," *Journal of Power Electronics*, vol. 19, no. 5, pp. 1278–1288, 2019, doi: 10.6113/JPE.2019.19.5.1278.
- [23] P. K. Maroti, R. Al-Ammari, A. Iqbal, L. Ben-Brahim, S. Padmanaban, and H. Abu-Rub, "A Novel High Gain Configurations of Modified SEPIC Converter for Renewable Energy Applications," *IEEE International Symposium on Industrial Electronics*, vol. 2019-June, pp. 2503–2508, 2019, doi: 10.1109/ISIE.2019.8781163.
- [24] K. S. Kavin and P. Subha Karuvelam, "PV-based Grid Interactive PMLBDC Electric Vehicle with High Gain Interleaved DC-DC SEPIC Converter," *IETE Journal of Research*, vol. 69, no. 7, pp. 4791–4805, 2023, doi: 10.1080/03772063.2021.1958070.
- [25] M. S. Nkambule, A. N. Hasan, and A. Ali, "MPPT under partial shading conditions based on Perturb & Observe and Incremental Conductance," *ELECO 2019 - 11th International Conference on Electrical and Electronics Engineering*, pp. 85–90, 2019.
- [26] R. K. Selvi and R. S. M. Malar, "A bridgeless Luo converter based speed control of switched reluctance motor using Particle Swarm Optimization (Pso) tuned proportional integral (Pi) controller," *Microprocessors and Microsystems*, vol. 75, p. 103039, 2020.
- [27] M. M. Reddy, P. S. Varma, and D. Lenine, "Improving gain of real time PI controller using particle swarm optimization in active power filter," *Microprocessors and Microsystems*, vol. 97, 2023, doi: 10.1016/j.micpro.2023.104760.
- [28] E. A. Mohamed Ali, A. Abudhahir, and A. Manivanna Boopathi, "Firefly algorithm tuned pi controller for pressure regulation in PEM fuel cells," *Journal of Computational and Theoretical Nanoscience*, vol. 15, no. 3, pp. 845–853, 2018, doi: 10.1166/jctn.2018.7164.
- [29] A. Zemmit, S. Messalti, and A. Harrag, "A new improved DTC of doubly fed induction machine using GA-based PI controller," *Ain Shams Engineering Journal*, vol. 9, no. 4, pp. 1877–1885, 2018, doi: 10.1016/j.asej.2016.10.011.
- [30] W. Boucheritte, A. Moussi, R. Mechoug, and H. Benguesmia, "A Multilevel Inverter for Grid-Connected Photovoltaic Systems Optimized by Genetic Algorithm," *Engineering, Technology and Applied Science Research*, vol. 13, no. 2, pp. 10249–10254, 2023, doi: 10.48084/etasr.5558.
- [31] A. Ahmad *et al.*, "Controller Parameters Optimization for Multi-Terminal DC Power System Using Ant Colony Optimization," *IEEE Access*, vol. 9, pp. 59910–59919, 2021, doi: 10.1109/ACCESS.2021.3073491.
- [32] A. H. Sule, A. S. Mokhtar, J. J. Bin Jamian, U. U. Sheikh, and A. Khidrani, "Grey Wolf Optimizer Tuned PI Controller for Enhancing Output Parameters of Fixed Speed Wind Turbine," *2020 IEEE International Conference on Automatic Control and Intelligent Systems, I2CACIS 2020 - Proceedings*, pp. 118–122, 2020, doi: 10.1109/I2CACIS49202.2020.9140171.
- [33] M. Fodil *et al.*, "Optimization of PI Controller Parameters by GWO Algorithm for Five-Phase Asynchronous Motor," *Energies*, vol. 16, no. 10, 2023, doi: 10.3390/en16104251.
- [34] M. M. Samy, M. I. Mosaad, and S. Barakat, "Optimal economic study of hybrid PV-wind-fuel cell system integrated to unreliable electric utility using hybrid search optimization technique," *International Journal of Hydrogen Energy*, vol. 46, no. 20, pp. 11217–11231, 2021.
- [35] F. Nejabatkhah, S. Danyali, S. H. Hosseini, M. Sabahi, and S. M. Niapour, "Modeling and control of a new three-input dc-dc boost converter for hybrid PV/FC/battery power system," *IEEE Transactions on Power Electronics*, vol. 27, no. 5, pp. 2309–2324, 2012, doi: 10.1109/TPEL.2011.2172465.
- [36] F. Galea, M. Apap, C. Spiteri Staines, and J. Cilia, "Design of a high efficiency wide input range isolated Cuk Dc-Dc converter for grid connected regenerative active loads," *World of Engineering Convention*, pp. 1–11, 2011.
- [37] P. Javeed, L. K. Yadav, P. Venkatesh Kumar, R. Kumar, and S. Swaroop, "SEPIC Converter for Low Power LED Applications," *Journal of Physics: Conference Series*, vol. 1818, no. 1, 2021, doi: 10.1088/1742-6596/1818/1/012220.

BIOGRAPHIES OF AUTHORS



Yannam Ravi Sankar    obtained his B.Tech. degree in electrical and electronics engineering from Prakasam Engineering College, Kadukur, JNTU Hyderabad, India in 2008. He obtained his M.Tech. degree in Power and industrial drives from NCET Vijayawada, JNTU Kakinada, India in 2011, and doing his Ph.D. at ANU University, Guntur, India. He is currently employed with Dire Dawa University, Institute of Technology, in Dire Dawa, Ethiopia, as a Lecturer in the Department of Electrical and Computer Engineering. His areas of interests are electrical machines, renewable energy sources, and power electronics. He can be contacted at email: ravi.yannam2@gmail.com.



Koritala Chandra Sekhar    graduated with honors in 1991 from V. R. Siddhartha Engineering College in Vijayawada, India with B.Tech. in electrical and electronics engineering, and in 1994 from Regional Engineering College in Warangal, India, with an M.Tech. in electrical machines and industrial drives. In 2008, he was awarded a Ph.D. by J.N.T.U. in Hyderabad, India. His research and teaching career spans 24 years. Presently, he holds positions of head of the Department of Electrical and Electronics Engineering and professor at the R.V.R. and J.C. College of Engineering in Guntur, India. His areas of interests are in research power electronics, industrial drives, and FACTS controllers. He can be contacted at email: cskoritala@gmail.com.